ISSN 1062-8738, Bulletin of the Russian Academy of Sciences: Physics, 2018, Vol. 82, No. 5, pp. 570–573. © Allerton Press, Inc., 2018.
Original Russian Text © I.I. Makoed, A.F. Ravinski, N.I. Gorbachuk, A.V. Pashchenko, N.A. Liedienov, A.A. Amirov, D.M. Yusupov, K.I. Janushkevich, 2018, published in Izvestiya Rossiiskoi Akademii Nauk, Seriya Fizicheskaya, 2018, Vol. 82, No. 5.

Structure and Dielectric Properties of $Bi_{0.80}Gd_{0.20-x}La_xFeO_3$ Multiferroics

I. I. Makoed[a, *], A. F. Ravinski[b], N. I. Gorbachuk[c], A. V. Pashchenko[d, e], N. A. Liedienov[d], A. A. Amirov[f, g], D. M. Yusupov[f], and K. I. Janushkevich[h]

[a] *Pushkin State University, Brest, 224016 Belarus*
[b] *Bialystok University of Technology, 15-001 Bialystok, Poland*
[c] *Belarusian State University, Minsk, 220030 Belarus*
[d] *Galkin Institute for Physics and Engineering, Donetsk, 83114 Ukraine*
[e] *Tugan-Baranovsky National University of Economics and Trade, Donetsk, 83050 Ukraine*
[f] *Amirkhanov Institute of Physics, Dagestan Scientific Center, Russian Academy of Sciences, Makhachkala, 367003 Russia*
[g] *Kant Baltic Federal University, Kaliningrad, 236041 Russia*
[h] *Scientific and Practical Materials Research Center, National Academy of Sciences of Belarus, Minsk, 220072 Belarus*
**e-mail: igmak2010@yandex.by*

Abstract—The structural and dielectric properties of $Bi_{0.80}Gd_{0.20-x}La_xFeO_3$ ($x = 0$–0.20) samples are studied by means of X-ray diffraction and dielectric spectroscopy. Room-temperature dielectric functions are examined experimentally at 1–10^{10} Hz. The dielectric properties are characterized theoretically using the Debye model with Cole–Cole and Cole–Davidson distributions of relaxation times. Correlations between structural parameters and dielectric properties are established.

DOI: 10.3103/S1062873818050210

Multiferroics are multifunctional materials that feature magnetic and electric ordering and are thus promising for application in modern spintronic devices [1]. Bismuth ferrite $BiFeO_3$ (BFO) holds a unique position among multiferroics, since ferroelectric and magnetic phases with high ordering temperatures ($T_C = 1083$ K, $T_N = 673$ K) coexist in it [2]. Bulk ceramic BFO samples exhibit antiferromagnetic properties due to a spatial spin-modulated structure with a period of 62 nm. The collapse of this structure establishes conditions for the emergence of a weak ferromagnetic moment and the magnetoelectric effect [3]. Different ways of suppressing the spin cycloid have been tested. One of these is to replace bismuth ions with isovalent cations of the lanthanide group (rare earths). Structural transformations induced by this substitution alter the physical parameters. The physical characteristics of complex ceramics based on bismuth ferrite are therefore of interest. The aim of this work was to examine the structural and dielectric properties of ceramic $Bi_{0.80}Gd_{0.20-x}La_xFeO_3$ ($x = 0$–0.20) samples.

The samples were synthesized via solid-phase reactions using the ceramic processing technology in [4]. The choice of substituting cations was due to the considerable difference between their magnetic moments and radii. This system is of interest in the context of high specific magnetization values found in $Bi_{1-x}Gd_xFeO_3$ [5], and because cation La^{3+} has a zero magnetic moment; the variation of magnetic properties of the $Bi_{0.80}Gd_{0.20-x}La_xFeO_3$ system is therefore governed by the magnetic properties of Gd^{3+}, since the radii of cations La^{3+} (1.16 Å) and Bi^{3+} (1.17 Å) are close [6]. It is also important that the electronic polarizability values of lanthanum and gadolinium cations differ considerably [7].

According to X-ray data, the isovalent replacing of Gd^{3+} with La^{3+} ions in $Bi_{0.80}Gd_{0.20-x}La_xFeO_3$ is accompanied by a structural phase transition from the rhombohedral structure ($R3c$) to the orthorhombic one ($Pnma$) at $x = 0.05$.

Figure 1 shows that $Bi_{0.80}Gd_{0.20-x}La_xFeO_3$ multiferroics exhibit ferroelectric properties. Open ferroelectric hysteresis loops were obtained for all three compositions. Saturation is not observed in the probed range of electric fields (from −100 to +100 kV/cm). $Bi_{0.80}La_{0.20}FeO_3$ has the greatest remanent polarization (1.12 μC/cm^2). Co-doping bismuth ferrite with La and Gd cations has an adverse effect on its ferroelectric properties: the residual polarization falls by 94% and 83% relative to that in $Bi_{0.80}La_{0.20}FeO_3$ and $Bi_{0.80}Gd_{0.20}FeO_3$, respectively. The coercive field

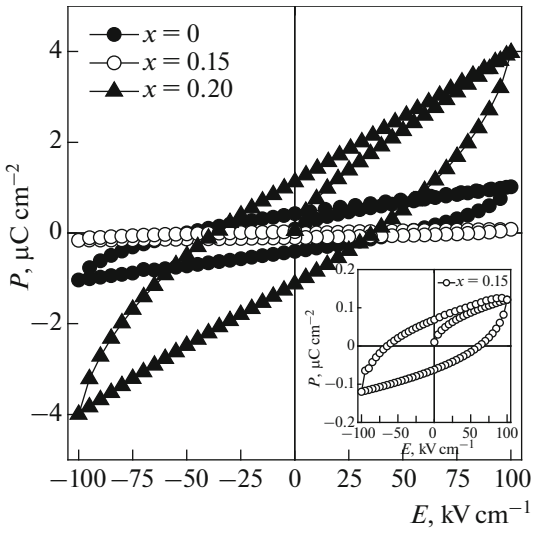

Fig. 1. Ferroelectric hysteresis loops $P(E)$ of $Bi_{0.80}Gd_{0.20-x}La_xFeO_3$ ($x = 0$, 0.15, 0.20) multiferroics.

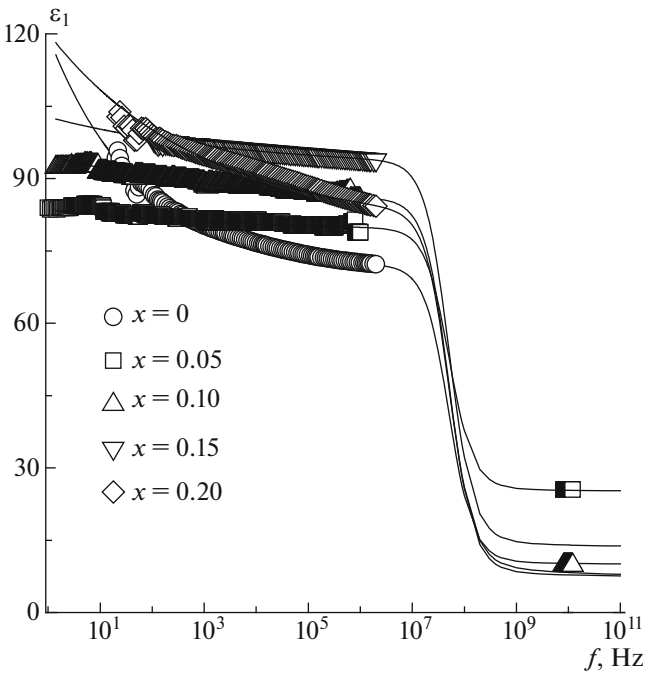

Fig. 2. Frequency dependences of the real permittivity component of the $Bi_{0.80}Gd_{0.20-x}La_xFeO_3$ ($x = 0$–0.20) samples. Solid curves represent model spectra.

strength depends weakly on the degree of substitution and varies from 30 to 50 kV/cm.

Figure 2 presents the dielectric properties of the samples measured via dielectric spectroscopy [8]. Static permittivity ε_{st} changes from 70 to 100 as the degree of substitution increases. The strongest dispersion of the real component of complex permittivity $\varepsilon^* = \varepsilon_1 + i\varepsilon_2$ (i.e., the highest rate of its reduction with an increase in frequency) is seen in the 10^7–10^9 Hz range. The high-frequency permittivity limit (ε_{HF}) determined at a frequency of 12 GHz varies from 10 ($x = 0$) to 25 ($x = 0.05$). Dielectric loss tangent $\tan\delta_\varepsilon = \varepsilon_2/\varepsilon_1$ falls monotonically with an increase in frequency and is independent of frequency in the $(1–1.3) \times 10^9$ Hz range. At room temperature, a steady-state ε_1 value, which may be considered a contribution established via electron and ion polarizations, is not achieved up to 10 GHz. This is because the relaxation mechanisms of dielectric polarization are still active in this frequency range. The obtained high-frequency limits exceed the values that could be associated with elastic electron and ion mechanisms.

Several mechanisms of dielectric polarization can be active in ionic oxide crystals at low (relative to optical) frequencies $f < 10^{10}$ Hz: electron jumps between identical crystallographic positions occupied by same-type ions of different valence; interlayer and intergrain polarization associated with the migration of weakly bound carriers and their accumulation at structural nonuniformities, defects, and grain boundaries; thermal ion polarization; orientation polarization of permanent dipoles; and polarization associated with the relaxation of walls of ferroelectric domains. The resonance frequencies of polarization mechanisms related to elastic displacements of electrons and ions fall within the infrared and optical spectral regions.

The following relations characterize the model spectra of ε^* components that agree fairly well with experimental data [9, 10]:

$$\varepsilon_1 = \varepsilon_{HF} + \frac{(\varepsilon_{st} - \varepsilon_{HF})[1 + (\omega\tau)^{1-\alpha}\sin(\pi\alpha/2)]}{1+2(\omega\tau)^{1-\alpha}\sin(\pi\alpha/2) + (\omega\tau)^{2(1-\alpha)}} + \frac{(\varepsilon_{st1} - \varepsilon_{HF1})[1 + (\omega\tau_2)^{\gamma}\sin(\pi\gamma/2)]}{1 + 2(\omega\tau_2)\sin(\pi\gamma/2) + (\omega\tau_2)^{2\gamma}} + \frac{\sigma_1}{\varepsilon_o\omega^{\beta_1}}, \quad (1)$$

$$\varepsilon_2 = \frac{(\varepsilon_{st} - \varepsilon_{HF})(\omega\tau)^{1-\alpha}\cos(\pi\alpha/2)}{1 + 2(\omega\tau)^{1-\alpha}\sin(\pi\alpha/2) + (\omega\tau)^{2(1-\alpha)}} + \frac{(\varepsilon_{st1} - \varepsilon_{HF1})(\omega\tau_2)^{\gamma}\cos(\pi\gamma/2)}{1 + 2(\omega\tau_2)\sin(\pi\gamma/2) + (\omega\tau_2)^{2\gamma}} + \frac{\sigma_2}{\varepsilon_o\omega^{\beta_2}}. \quad (2)$$

Here, ε_{st} is static permittivity and ε_{HF} is its high-frequency limit. Parameter α characterizes the distributions of relaxation times τ, which in the first approximation are determined from condition $\omega_{max}\tau = 1$ (where ω_{max} is the frequency corresponding to the $\tan\delta_\varepsilon$ maximum). The second and third terms are mathematical expressions characterizing the Debye model with Cole–Cole and Cole–Davidson distributions of relaxation times [9, 10], respectively, and model the relaxation behavior of dielectric functions in different frequency intervals.

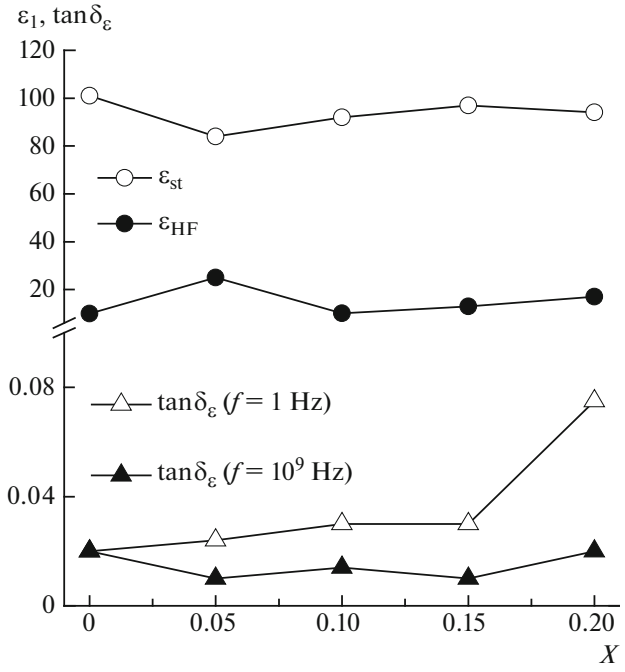

Fig. 3. Concentration dependences of the real component of permittivity and the dielectric loss tangent of the $Bi_{0.80}Gd_{0.20-x}La_xFeO_3$ ($x = 0$–0.20) samples.

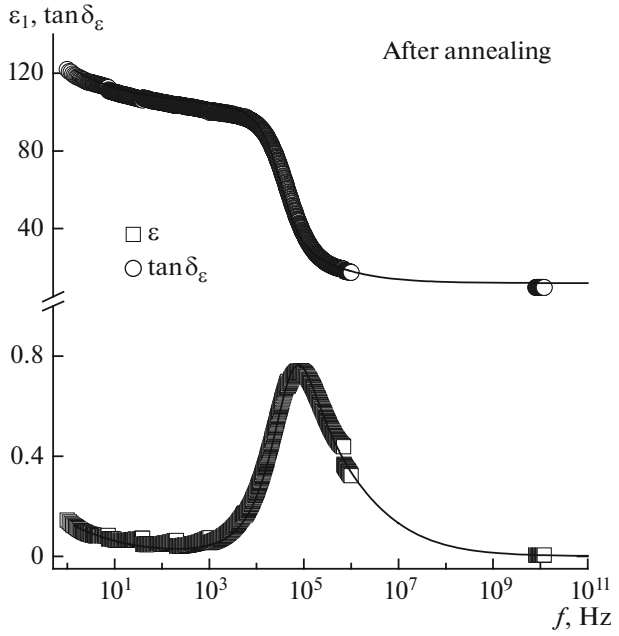

Fig. 4. Concentration dependences of the real component of permittivity and the dielectric loss tangent of the $Bi_{0.80}Gd_{0.10}La_{0.10}FeO_3$ sample measured after additional annealing. Solid curves represent model spectra.

The second term in (1) is associated with the jump mechanism of electron exchange between Fe^{2+} and Fe^{3+}, which is active in the range of 10^3 to 10^6 Hz [11–13]. The emergence of aliovalent iron ions was confirmed by XPS data in [14]. The third term in (1) characterizes the high-frequency relaxation mechanism of dielectric polarization. Its nature has not been established conclusively. The probable mechanism of dielectric polarization in the 10^7–10^9 Hz range is the displacement of walls of ferroelectric domains [12]. The behavior of permittivity in this frequency interval can also be interpreted within the model of improper ferroelectric polarization associated with the production of electric dipoles due to the displacement of ions under the influence of an external electric field.

In the low-frequency limit, which is characterized by the last term in (1), large $\tan\delta_\varepsilon$ values are established by the contributions from quasi-free current carriers to dielectric polarization; i.e., dielectric losses are related to conductivity in accordance with the Maxwell–Wagner and Koops models [15, 16]. Expressions (1) and (2) allow us to obtain model spectra that differ from experimental ones by a value lower than the experimental error over the range of frequencies. The concentration dependences of components of permittivity and dielectric loss tangents measured at the boundaries of the studied intervals are shown Fig. 3. The values of ε_1 increase somewhat in the $0.10 < x < 0.20$ range. The nonmonotonic behavior of ε_1 at $x = 0.05$ is attributable to the structural phase transition. Magnetic interactions are also likely to affect the dielectric properties [4].

To examine the effect the conditions of synthesis have on the dielectric functions (see Fig. 4), the samples were subjected to isothermal ($t = 730$°C) annealing in air for 18 h. It is likely that the increase in the number of Fe^{2+} cations observed after annealing was accompanied by the growth of vacancy-type defects [14]. The presence of such defects led to pinning of the walls of ferroelectric and magnetic domains and thus to suppression of the contribution associated with the displacement of domain walls. At the same time, dielectric losses grew in the 10^4–10^6 Hz range, and the distribution of relaxation times τ narrowed. Relative permittivity ε_1 and dielectric loss tangent $\tan\delta_\varepsilon$ for the $Bi_{0.80}Gd_{0.10}La_{0.10}FeO_3$ samples increased by 23 and 79% in the low-frequency limit after annealing (see Figs. 3 and 4).

ACKNOWLEDGMENTS

This work was performed as part of the government research program “Physical Materials Science, New Materials and Technology for 2016–2020” (subprogram “Materials Science and Technology,” project no. 1.35). Some of the results reported above were obtained with partial support from the Ukraine State Fund for Fundamental Research, project no. F71/46-2017.

REFERENCES

1. Opel, M., *J. Phys. D*, 2012, vol. 45, p. 033001.
2. Catalan, G. and Scott, J.F., *Adv. Mater.*, 2009, vol. 21, p. 2463.
3. Park, J.G., Le, M.D., Jeong, J., and Lee, S., *J. Phys.: Condens. Matter*, 2014, vol. 26, p. 433202.
4. Makoed, I.I., Anishchik, V.M., Revinskii, A.F., et al., in *Trudy XIX Mezhdunarodnogo mezhdistsiplinarnogo simpoziuma "Poryadok, besporyadok i svoistva oksidov"* (Proc. XIX Int. Symp. "Order, Disorder, and Properties of Oxides"), Rostov-on-Don, 2016, p. 105.
5. Lazenka, V.V., Zhang, G., Vanacken, J., et al., *J. Phys. D*, 2012, vol. 45, p. 125002.
6. Shannon, R.D., *Acta Crystallogr.*, 1976, vol. A32, p. 751.
7. Zhao, X., Wang, X., Lin, H., and Wang, Z., *Phys. B*, 2007, vol. 392, p. 132.
8. Tatarchuk, D.D., Molchanov, V.I., and Pashkov, V.M., in *Proc. 35th IEEE Int. Conf. on Electronics and Nanotechnology*, Kyiv, 2015, p. 231.
9. Cole, K.S. and Cole, R.H., *J. Chem. Phys.*, 1941, vol. 9, p. 341.
10. Davidson, D.W. and Cole, R.H., *J. Chem. Phys.*, 1951, vol. 19, p. 1484.
11. Makoed, I.I. and Danil'kevich, M.I., *Inorg. Mater.*, 1998, vol. 34, no. 7, p. 737.
12. Cheng, Z., Wang, X., and Dou, S.X., *J. Appl. Phys.*, 2008, vol. 104, p. 116109.
13. Pashchenko, A.V., Tatarchuk, D.D., and Liedienov, N.A., in *Proc. 36th IEEE Int. Conf. on Electronics and Nanotechnology*, Kyiv, 2016, p. 107.
14. Pashchenko, A.V., Liedienov, N.A., Prokopenko, V.K., et al., in *Proc. 19th. Int. Conference–School "Advanced Materials and Technologies,"* Palanga, 2017, p. 93.
15. Maxwell, J.C., *A Treatise on Electricity and Magnetism*, Oxford: Clarendon, 1873, vol. 1.
16. Koops, C.G., *Phys. Rev.*, 1951, vol. 83, no. 1, p. 121.

Translated by D. Safin